SHORT COMMUNICATION

Anchoring of polyacrylate onto silica and formation of polyacrylate/silica nanocomposite particles via in situ emulsion polymerization

Dong-ming Qi · Yong-zhong Bao · Zhi-ming Huang · Zhi-xue Weng

Abstract Polyacrylate/silica nanocomposite latex particles were prepared by in situ emulsion polymerization of acrylate monomers initiated by 2,2′-azobis(2-amidinopropane)-dihydrochloride (AIBA) adsorbed by silica nanoparticles. The anchoring of polyacrylate (ACR) onto silica nanoparticles was achieved through the physical absorption and chemical grafting reaction. The elution and HF etching experiments showed that most silica nanoparticles were encapsulated by ACR to form the raspberry-like ACR/silica nanocomposite latex particles. The silica nanoparticles with a greater grafting degree of ACR tended to locate in the bulk of the polymer, and the silica particle with a lower grafting degree would not be combined with polymer latex particles and always remained in water phase. The formation of the final ACR/silica nanocomposite latex particles included the anchoring of ACR onto silica primary particles, aggregation of silica primary particles to form the silica-containing latex particles, and the growth of latex particles.

Keywords Emulsion polymerization · Acrylate · Nanocomposite · Anchoring

Introduction

During the past two decades, much attention has been paid to the preparation of polymer/inorganic nanoparticle composites due to their attractive mechanical [1–5], thermal [6, 7], optical [8], electrical [9], and magnetic [10] properties and potential application in fields of plastics and rubber reinforcement, coatings, electronics, catalysis, and diagnostics.

The final properties of polymer/inorganic particle nanocomposites greatly depend on both the dispersing degree of nanoparticles in the base polymers and the interfacial adhesion between the inorganic and organic components. The surface coating of inorganic nanoparticles with polymer, via emulsion polymerization, is regarded as a useful approach to increase the dispersing ability and interfacial adhesion simultaneously [11, 12]. However, as the inorganic particles are added into the emulsion polymerization system, the particle surface can become an additional site for particle nucleation except the principal locus of the aqueous phase or the monomer-swollen micelles. To improve the coating efficiency of polymer onto inorganic particles, two main strategies are used solely or conjunctly, one, introducing initiator [13–16], coupling agents [12, 17–21] or macromonomer [22] onto the surface of nanoparticles, and the other, applying an auxiliary monomer [23–25] or a special surfactant [26–28] in the emulsion polymerization process. Thus, a series of nanocomposite particles with core-shell [14, 19–21], raspberry-like [13–15, 25–27], daisy-shape [12, 22], guava-like [20, 24, 25], and multipod-like [12, 28] morphologies can be obtained depending on the formation mechanism as well as the surface chemistry and the size of inorganic particles [19, 20, 23, 25, 29].

D.-m. Qi · Y.-z. Bao (✉) · Z.-m. Huang · Z.-x. Weng
State Key Laboratory of Chemical Engineering,
Zhejiang University,
Hangzhou 310027, China
e-mail: yongzhongbao@zju.edu.cn

D.-m. Qi
Key Laboratory of Advanced Textile Materials and Manufacturing Technology, Ministry of Education, Zhejiang Sci-Tech University, Hangzhou 310018, China

Silica nanoparticles are widely used in the preparation of polymer nanocomposites due to their versatility. When the pH value of the water phase is greater than the isoelectric potential of silica (pH=3.7), the silica particles would be hydrated in water and exhibit the negative charges [13]. Thus, it is a facile and effective way to introduce an initiator-containing cationic group(s) onto the surface of silica particles through an electrostatic attraction, and then, to prepare polymer/silica nanocomposite particles via in situ polymerization initiated by the absorbed initiator on silica particles. Luna-Xavier et al. [14, 15] prepared the raspberry-like silica/poly(methyl methacrylate) (PMMA) composite particles via emulsion polymerization initiated by the adsorbed 2.2′-azobis(2-amidinopropane)dihydrochloride (AIBA) on silica particles with size of 70–200 nm. They found that the electrostatic attraction between both types of particles was taking place either in situ by reacting AIBA in the presence of silica or ex situ by mixing the silica and preformed PMMA latexes, especially that the former was crucial to achieve a high coating efficiency of PMMA on silica particles.

In our previous paper [30], the adsorption behavior of AIBA onto the surface of silica particles with a size of about 15 nm and the synthesis of polyacrylate/silica nanocomposite particles via in situ emulsion polymerization were investigated. In the present paper, the anchoring of polyacrylate (ACR) on the silica particles and the combination degree of silica particles with ACR latex particles in the composite latexes were investigated to illustrate the formation mechanism of ACR/silica nanocomposite particles during in situ emulsion polymerization.

Experimental

Materials

Silica aqueous dispersion (30 wt% solid content) was supplied by Yuda Chemical, Zhejiang, China. The size of silica particles was about 15 nm, determined by dynamic light scattering on a Zetasizer 3000HS particle size analyzer (Malvern Instruments, Laramie, USA) and a JSM-1230EX type transmission electron microscopy (JEOL, Japan). Commercial butyl acrylate (BA, Dongfang Chemical, Beijing, China) and methyl methacrylate (MMA, Gaoqiao Chemical, Shanghai, China) were distilled under reduced pressure before polymerization. 2.2′-azobis(2-amidinopropane)dihydrochloride (AIBA) with analytical purity, were obtained from Acros Organics. Nonionic surfactant nonylphenol poly(oxyethylene) (C_9H_{19}-⟨⟩-(O-CH_2-CH_2)$_{10}$-OH, OP-10) was purchased from Anli Chemical Factory (Suzhou, China). Sodium dodecyl sulfate (SDS), with analytical purity, was purchased from Shanghai No. 2 Chemistry Reagent. Hydrofluoric acid

(HF, 30 wt%) was supplied by Juhua Group (Quzhou, China). Ammonia water solution and acetone were used as received.

Preparation of ACR/silica composite latex

The absorption of AIBA onto silica particles was conducted at 25 °C under a N_2 atmosphere [30]. The polymerizations were carried out in a 200-ml jacketed glass reactor fitted with a condenser, a N_2 inlet, a thermometer, and a paddle-type agitator. In a typical polymerization procedure, the reactor was charged with deionized water, the dispersion of silica absorbed with AIBA, and the nonionic surfactant OP-10. The pH value of the mixture was adjusted to 10 by adding ammonia aqueous solution, and the mixture was gently agitated for 10 min under ambient temperature. Then, the temperature of the mixture in the reactor was raised to 70 °C, and a certain amount of MMA/BA mixed monomers (MMA/BA=3/1 in weight) was added to start the polymerization. The polymerization was conducted for 5 h under a N_2 atmosphere. The recipes for the preparation of ACR/silica nanocomposite particles (S2~S7) are shown in Table 1. SDS solution was added when the emulsion polymerization had proceeded for 3 h.

For comparison, an ACR latex without silica (S1) was prepared via a conventional emulsion polymerization process by using of AIBA initiator. The ACR + silica composite latex (S1a) was prepared by the direct mixing of ACR latex (S1) with the silica aqueous dispersion for 2 h.

Characterization

Polymerization conversion

The latex samples were collected during in situ emulsion polymerization process, and the conversions of MMA and BA to polymer (X) were determined gravimetrically.

Table 1 Recipes for conventional emulsion polymerization of MMA/BA and in situ emulsion polymerizations of MMA/BA in the presence of AIBA adsorbed silica particles

Ingredients (g)	S1	S2	S3	S4	S5	S6	S7
H_2O (pH=10)	88.0	87.1	84.4	84.4	84.4	84.4	80.8
SiO_2	–	0.9	3.6	3.6	3.6	3.6	7.2
MMA	9.0	9.0	9.0	9.0	9.0	9.0	9.0
BA	3.0	3.0	3.0	3.0	3.0	3.0	3.0
OP-10	0.20	0.20	0.20	0.20	0.20	0.20	0.20
SDS	0.044	0.044	0.044	0.044	0.044	0.044	0.044
AIBA	0.20	0.05	0.05	0.10	0.15	0.20	0.40

Distribution of silica particles in composite latex

To determine the distribution of silica particles in the composite latex, two steps, including an elution process and a HF etching process, were applied.

(1) A certain amount of composite latex was centrifuged at 12,000 r min^{-1} and at room temperature for 60 min to form a serum and a deposit. The deposit was dispersed into an ammonia solution (pH=10, containing 0.2 wt% OP-10, and the mass was similar to that of the separated serum) by magnetic stirring for 60 min after separation of the serum. The dispersion was centrifuged, and the serum was separated again. This elution process was repeated five times to achieve a complete separation of the silica particles remaining in aqueous phase (defined as the free silica particles) from the composite latex particles. All serums and the final deposit were collected, respectively. The serums were dried at 120 °C for 12 h and thermal treated in an electric muffle furnace at 600 °C for 5 h to remove water and organic substance. The weight of silica in all collected serums was measured, and the weight percent of free silica to total silica added could be calculated.

(2) A certain amount of the composite latex was slowly added into an excess HF solution. All free silica particles in aqueous phase and all silica particles attached to ACR phase at the water/organic interface (defined as the incompletely encapsulated silica particles) would be etched by HF acid [31]. The final residual was collected at once, neutralized by the ammonia solution, vacuum dried at 150 °C for 12 h and then thermal treated in the electric muffle furnace at 600 °C for 5 h. The residual silica is defined as the completely encapsulated silica, and its weight percent to the total silica could be determined gravimetrically.

Combining the results of step 1 and step 2, the weight percent of incompletely encapsulated silica could also be obtained.

Grafting degree and grafting efficiency of ACR on silica particles

The grafting degree of ACR (GD) on the silica particles was defined as the weight percentage of grafted ACR onto the silica to the total added silica. The grafting efficiency (GE) of ACR was defined as the weight percentage of grafted ACR to the total formed ACR.

The ACR/silica composite latexes collected at the different polymerization times (different polymerization conversions) were dried and extracted with acetone for 24 h to remove free ACR polymer. The weight percents of C and H

elements of the dried residual were determined by an elemental analysis (Flash EA1112, ThermoFinnigan, Italy). The grafting degree of ACR on silica particles was calculated according to Berendsen equation [32]. The grafting efficiency of ACR could be calculated as follows:

$$GE = \frac{GD \bullet W_{SiO_2}}{W_{monomer} \bullet X} \quad (1)$$

where W_{SiO_2} is the weight of silica added in polymerization, $W_{monomer}$ the weight of added MMA and BA, and X, the conversion of MMA and BA to polymer.

The grafting degrees of ACR on the free silica and on the completely encapsulated silica in the final composite were measured by the same method. The grafting degree of ACR on the incompletely encapsulated silica was calculated in considering the silica distribution, the average grafting degrees of ACR in the final composite and the grafting degrees of ACR on the free silica and on the completely encapsulated silica.

Morphology of ACR/silica composite particles

The morphology of ACR/silica composite latex was directly observed by using a TEM-1230EX type transmission electron microscope (TEM) (JEOL Japan).

The S1a composite latex and S6 ACR/silica nanocomposite latex particles were coagulated, separated from water, and dried. The dried composites were blended with pure ACR powder and melt-pressed at 170 °C and 30 MPa to form molded samples. The molded composites were sliced using an ultra-microtome (Reichert-Jung ULTRA-CUT E, Austria), and the morphology of ACR/silica composites was observed by using the same TEM device.

*Size distribution of silica particles and latex particles*

The size distribution of the silica particles absorbed with AIBA and the latex samples collected during in situ emulsion polymerization were determined by dynamic light scattering on a Zetasizer 3000 HS particle size analyzer (Malvern Instrument USA) using a saturated aqueous solution of OP-10 (pH=10) as a diluting agent.

Results and discussion

Anchoring of ACR onto silica particles

It was evidenced that the AIBA initiator added into the silica aqueous dispersion can be stably adsorbed onto the silica with a great absorption efficiency via the electrostatic interaction when the pH value of the medium was kept at 10 [30]. As the polymerization temperature achieved, the

absorbed AIBA molecules were thermal decomposed to produce the absorbed and separated free radicals as follows:
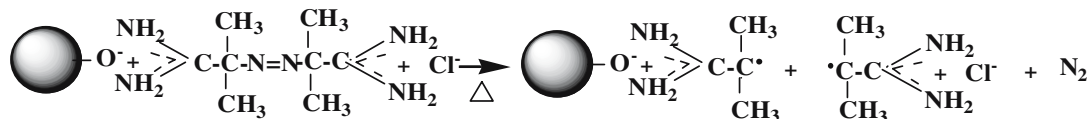
The polymerization started as the acrylate monomers initiated by the above free radicals.

The conversions of S2~S7 runs, and the weight percents of silica in the final composite latexes (based on polymer) were measured and are shown in Table 2. It can be seen that the conversion increased as more AIBA was added when the weight percent of silica in feed was kept at constant (S3~S6). The conversion also increased as more silica was added in polymerization (S2, S6, and S7), when the ratio of AIBA to silica was kept constant. The above results were caused by the increased AIBA concentration in the polymerization system.

The polymerization initiated by the absorbed free radicals would lead to the formation of ACR physically absorbed by silica nanoparticles. The ACR polymer chains formed through the initiation of the separated free radicals contained cationic end group(s) and were partially absorbed by silica nanoparticles. It was expected that the most ACR chains would be physically absorbed by silica nanoparticles, although the direct determination of the amount of ACR absorbed was very difficult.

Through the solvent extraction of ACR/SiO$_2$ composites (S2~S7) and the element analysis of the extraction residue, it was found that some non-extractable polymer existed in the S2~S7 composites, indicating chemical grafting of ACR polymer onto silica nanoparticles. The existence of non-extractable polymer was also observed by Luna-Xavier et al. [13], and it was explained that the transfer and termination reaction occurring on active sites formed on silica were responsible for the formation of the tightly

bonded polymer. Thus, it is considered that the anchoring of ACR polymer onto silica was achieved through two ways: physical absorption and chemical grafting reaction.
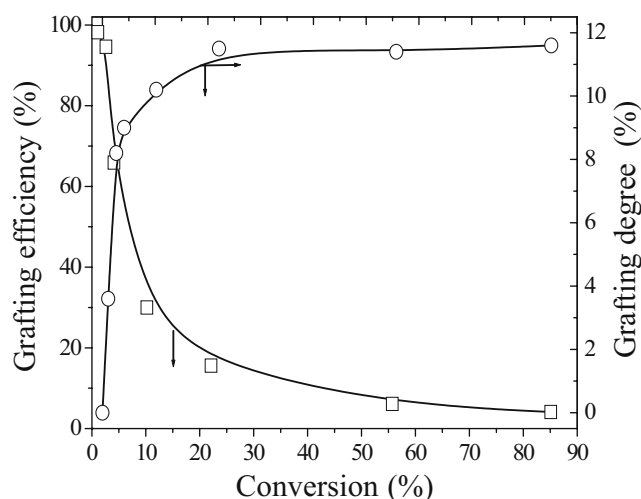
The grafting degree (GD) and grafting efficiency (GE) of ACR on silica of the final composites are also shown in Table 2. Comparing on Run S3~S6, in which the weight fraction of silica in feed was fixed and the usage of AIBA increases from 0.05 to 0.20 mmol/g SiO$_2$, it can be seen that the GE of ACR changes no more, and GD increases as the usage of AIBA increases. The increased GD of ACR was related with the increased polymerization conversion when more AIBA was added and absorbed onto silica. Comparing on Run S2, S6, and S7, it can be seen that the GD changes no more, and the GE increases as the weight fraction of silica increases when the usage of AIBA is kept at 0.20 mmol/g SiO$_2$. It is expected that more active sites would be formed as the weight fraction of silica increased, which would be favor to the grafting of ACR onto silica particles.

The grafting behavior of ACR onto the silica particles was further investigated in view of the evolvement of GD and GE of ACR with the polymerization conversion (X). The result is shown in Fig. 1.

It can be seen that the GD of ACR increases rapidly when the conversion is lower than 20% and gradually

**Table 2** Conversion, weight percent of silica, GD, and GE of ACR for S2~S7 runs

Run	AIBA usage (mmol/g SiO$_2$)	Weight percent of SiO$_2$ in feed (%)	Conversion (%)	Weight percent of SiO$_2$ in product (%)	GD (%)	GE (%)
S2	0.20	7.0	82.0	8.5	12.6	1.1
S3	0.05	23.1	60.2	38.4	7.1	2.7
S4	0.10	23.1	74.5	31.0	9.9	3.1
S5	0.15	23.1	82.6	28.0	10.5	2.9
S6	0.20	23.1	85.7	27.0	11.4	3.1
S7	0.20	37.5	90.0	41.6	11.6	4.8

Fig. 1 Variation of grafting degree and grafting efficiency of ACR with polymerization conversion for in situ emulsion polymerization of Run S6

Fig. 2 Typical TEM micrographs of pure ACR latex particles (S1), ACR + silica composite latex particles (S1a, 25.1 wt% silica) and ACR/silica nanocomposite particles prepared by in situ emulsion polymerization (S2 8.5 wt%, S6 27.0 wt%, and S7 41.6 wt% silica)
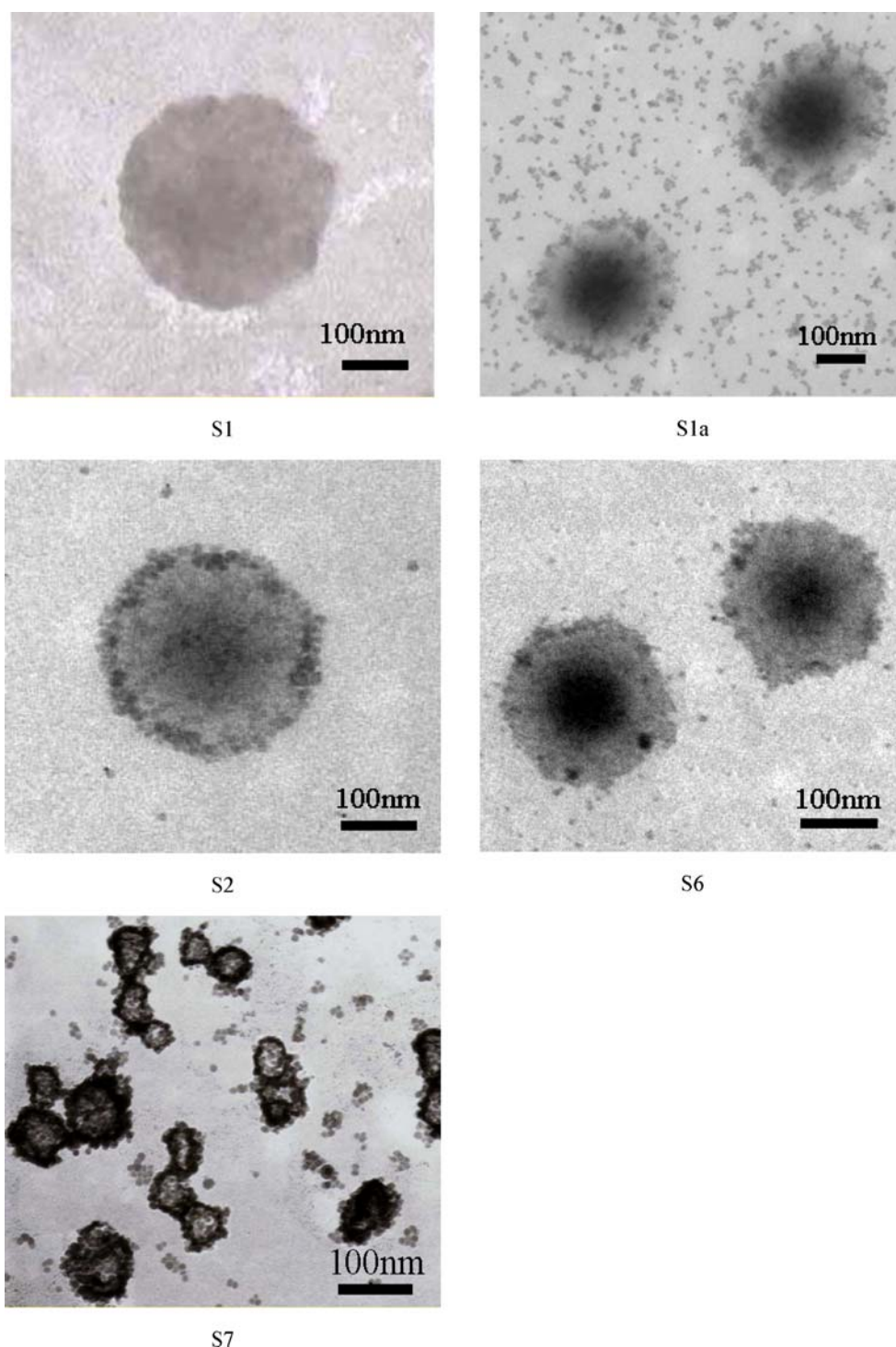
levels off when the conversion exceeds 20%, while the GE of ACR gradually decreases with the increase of conversion. This indicated that the grafting of ACR on silica particles occurred at the early stage of polymerization, in which the surface of silica particles are easily attacked by free radicals to form the active sites, and the monomers are easy to contact with the active sites to form grafted polymer chains. As more grafted and physically absorbed polymers

Table 3 Distribution of silica particles in the ACR/silica composite latexes

	S1a	S2	S6	S7
Weight percent of silica in latex (%)	25.1	8.5	27.0	41.6
Weight percent of				
Completely encapsulated silica (%)	0	35.3	32.8	25.5
Incompletely encapsulated silica (%)	33.3	63.8	63.3	55.9
Free silica (%)	66.7	0.9	3.9	18.6

Table 4 Grafting degree of ACR on silica particles with different combination degree with ACR latex particles

Silica type	GD of ACR on silica particles (%)
Free silica	1.5
Completely encapsulated silica	16.8
Incompletely encapsulated silica	13.4

are formed at the surface of silica particles, the grafting reaction is hindered, while the physical coating of polymer on silica particles continues.

Combination condition of silica particles with ACR latex particles in composite latexes

Typical TEM micrographs of pure ACR particles (S1), ACR + silica composite particles (S1a) and ACR/silica nanocomposite particles prepared by in situ emulsion polymerization (S2, S6, and S7) are presented in Fig. 2.

It can be seen from TEM micrographs that ACR/silica nanocomposite particles have a raspberry-like morphology with most silica particles existing at the surface of latex particles. It can also be seen that the continuous phase of the nanocomposite latexes is far clearer than that of ACR + silica composite latex with a near weight fraction of silica. Thus, it can be concluded that most silica particles have been combined with latex particles via in situ emulsion polymerization.

The silica particles in the nanocomposite latexes were possibly distributed as the free silica in the aqueous phase, attached silica particles located at the surface of polymer latex particles (incompletely encapsulated silica particles), and encapsulated silica in the bulk of the polymer latexes (completely encapsulated silica particles). The free silica particles exhibited the strong electrostatic repulsion to resist centrifugal force, so they can still be dispersed in aqueous phase during the centrifugation process and be separated from the composite latex by the elution process. The attached silica particles and the encapsulated silica particles can be distinguished by applying the HF etching method [31].

Combining the elution and etching results, the combination condition of silica particles with ACR latex particles was illustrated. The results of ACR/silica nanocomposite latexes with different silica contents are compared with that of ACR + silica composite latex in Table 3.

It can be seen that two out of three silica particles are dispersed in the water phase for ACR + silica composite latex, while about 60 wt% silica particles are attached at the surface of polymer latex particles, and about 30 wt% silica particles are encapsulated in the bulk of the polymer latex particles for ACR/silica nanocomposite latexes, although

the weight percent of free silica increases as the weight percent of silica increased. It indicates that the adsorption of initiator on silica particles before the addition of monomers and surfactant would significantly increase the combination degree of silica with polymer latex particles.

Grafting degree of ACR on silica particles with different combination degree with ACR latex particles

For the final product of S7 (weight percent of silica is 41.6%), the average GD of ACR on all silica particles, the GD of ACR on the free silica and on the completely encapsulated silica was measured, respectively. The GD of ACR on the incompletely encapsulated silica was calculated by applying the mass balance. The result is listed in Table 4.

It can be seen that the combination condition of silica particles strictly relates with the grafting degree of ACR on silica particles. The silica particles with more grafted ACR could be encapsulated in the bulk of composite particles, and the silica particles with less grafted ACR always dispersed in the water phase, while the incompletely encapsulated silica particles exhibited a mediate grafting degree of ACR.

Evolvement of particle size distribution during in situ emulsion polymerization

Taking Run S6 as an example, the variation of particle size distribution during in situ emulsion polymerization is shown in Fig. 3. It can be seen that silica particles are still well dispersed in aqueous phase as AIBA added, as the usage of AIBA was below the critical value for the stable dispersion of silica [30]. After the addition of the acrylate
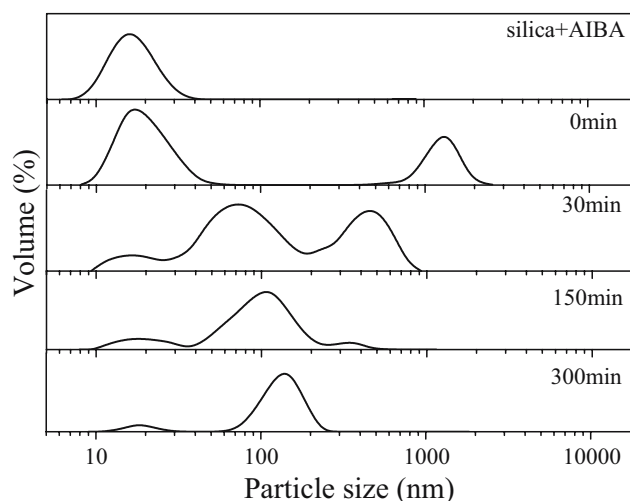
Fig. 3 Variation of particle size distribution during in situ emulsion polymerization (Run S6)

monomers and OP-10 emulsifier, two peaks appear in the distribution curve. The peak with a low average size is formed by silica particles with a part of absorbed OP-10 and swollen monomers. The peak with a great average size corresponded to the monomer droplets with a few of silica particles absorbed on the surface of droplets acting as a pickering emulsifier [33]. As polymerization proceeded, the third peak with a mediate average size and corresponding to the latex particle appears in the distribution curve. As polymerization time (conversion) increases, the volume fraction of latex particles increases, while the volume fractions of silica particles and the monomer droplets decrease. Finally, the monomer droplets completely disappeared, and the ACR/silica nanocomposite latex containing a low volume fraction of free silica particles is formed.

## Formation mechanism of ACR/silica nanocomposite particles

According to the above anchoring behavior of ACR on silica particles, the combination condition of silica particles with ACR latex particles in the composite latexes and the variation of particle size distribution during in situ emulsion polymerization, a possible formation mechanism of the raspberry-like ACR/silica nanocomposite latex particles, was proposed, and the scheme is shown in Fig. 4.

In this case, the added AIBA was mainly absorbed on silica primary particles, and the free radicals produced can still be absorbed by silica particles. Thus, at the early stage of polymerization, the surface of silica primary particles

became the main polymerization locus, and the physical absorption and chemical grafting of ACR polymer onto silica particles took place simultaneously.

As silica particle is hydrophilic, and the monomers are hydrophobic, the diffusion of monomers from water phase or monomer droplets to silica surface is difficult and becomes the control step in the further polymerization. The silica particles with more physically absorbed and chemically grafted ACR can be further anchored with more polymer than those with less anchored polymer, as the anchored polymer can improve the ability of silica particles to absorb the monomers. As more and more ACR anchored (encapsulated) onto the silica primary particles, the hydrophilicity and the colloidal stability of silica particles decreased, and the encapsulated silica particles trended to aggregate to form silica-containing latex particles. Thus, the silica-containing latex particles became the main locus of polymerization and grew in size due to their great monomers and free radical capture abilities. Especially, the silica particles with more physical absorbed and chemical grafted ACR can be coated by ACR from whole surface of silica particles and be tied into the internal of latex particles, acting as the completely encapsulated silica particles. The silica particles with a mediate anchoring degree of ACR would be partially coated by ACR and finally be attached at the surface of composite particles. Thus, the raspberry-like ACR/silica nanocomposite particles were formed as shown in Fig. 4. During the AIBA absorption process, silica primary particles with less absorbed AIBA would also be formed. Thus, less ACR would be anchored onto these silica primary particles, and

Fig. 4 Schematic diagram of formation mechanism of raspberry-like ACR/silica nanocomposite particles
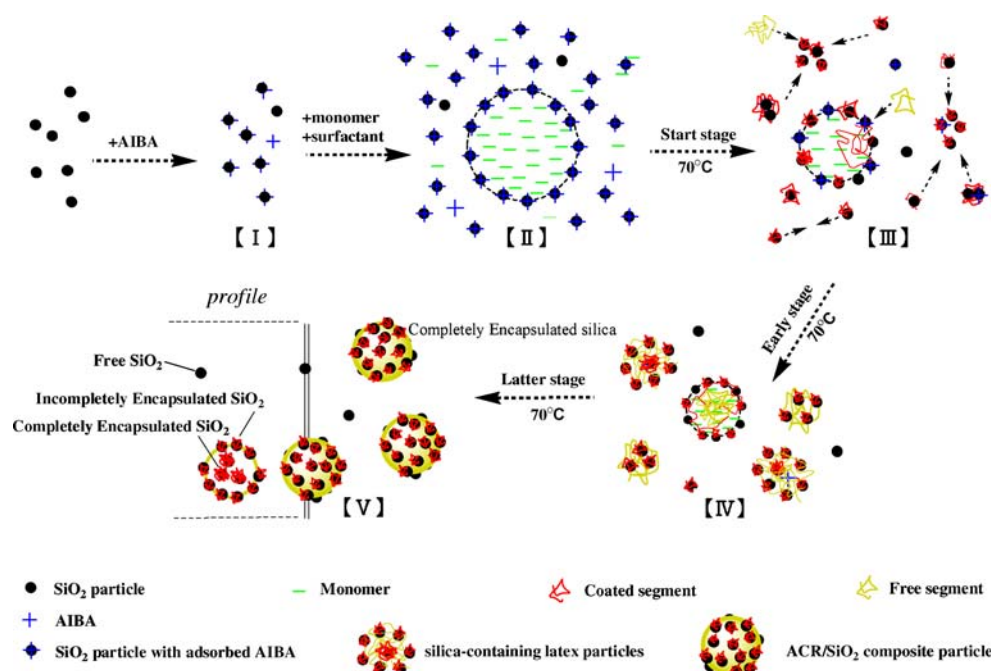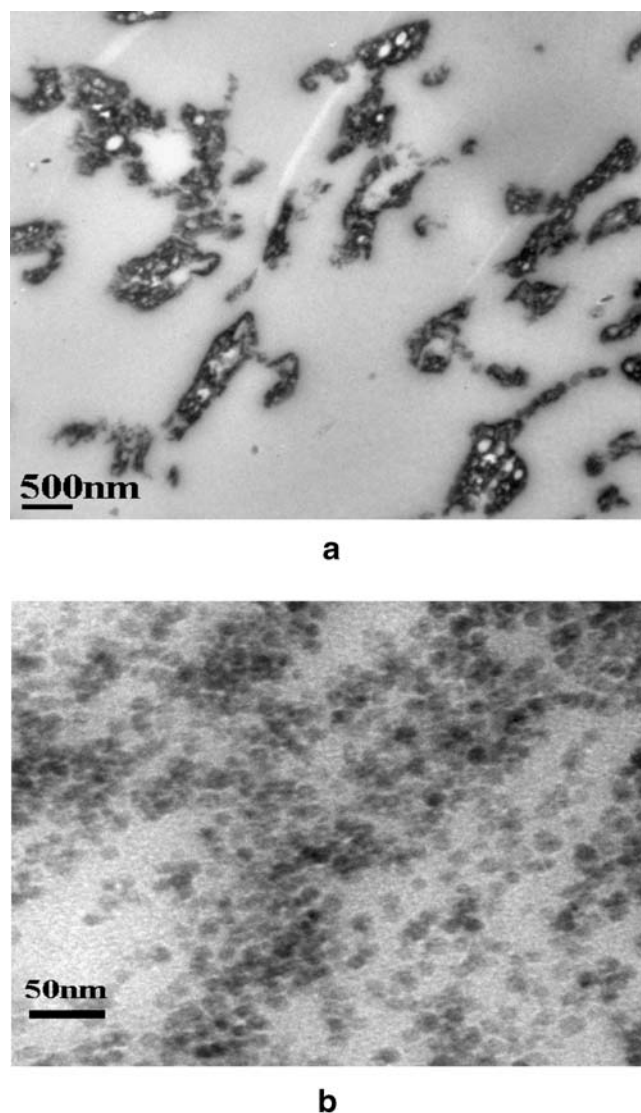
Fig. 5 TEM micrographs of ACR/silica composite prepared by melt-processing of S1a and pure ACR (**a**), and of S6 and pure ACR (**b**), (weight fraction of silica in the final composites is 15%)

they would still be hydrophilic and be dispersed in the water phase as the free silica.

The dispersing ability of silica nanoparticles in polymer matrix and their affinity with polymer would be improved as ACR anchored onto them. ACR/silica composites prepared by the direct mixing (S1a) and by in situ emulsion polymerization (S6) were melt-processed with pure ACR to obtain the molded ACR/silica composites with a near silica weight fraction (15.0%), and the TEM micrographs of the sliced samples are shown in Fig. 5. It can be seen that the silica particles are seriously aggregated in ACR composite prepared from S1a and pure ACR, while the silica particles are well dispersed in the ACR composite prepared from S6 and pure ACR. So, in situ emulsion polymerization is an effective approach to synthesize ACR latex particles containing silica nanoparticles with a well-dispersing ability.

Conclusions

A series of raspberry-like ACR/silica nanocomposite particles with different weight fractions of silica particles were successfully prepared by in situ emulsion polymerization. During the in situ emulsion polymerization process, the physical absorption and chemical grafting of ACR onto silica particles took place simultaneously, and the silica particles were gradually combined with polymer to form the composite latex particles. In the ACR/silica nano-composite latex, about 60% silica particles with about 13.4% grafted ACR were attached at the surface of composite latex particles, about 30% silica particles with about 16.8% grafted ACR were encapsulated in the inner of composite latex particles, and other silica particles with less grafted polymer were dispersed in the aqueous phase. It was proposed that the surface of silica particles acted as the main reaction loci at the start stage of polymerization, while the silica-containing latex particles acted as the main reaction loci in the latter stage.

In summary, it is the effective and strong electrostatic adsorption of initiator on the silica particles that markedly improve the probability of anchoring of ACR onto the surface of silica particles and the combination degree of silica particles with polymer latex particles. Of course, further investigation should be done to disclose the essential grafting mechanism of ACR onto silica particles.

References

1. Fröhlich J, Niedermeier W, Luginsland HD (2005) Composites Appl S 36:449
2. Bandyopadhyay A, De Sarkar M, Bhowmick AK (2005) J Appl Poly Sci 95:1418
3. Odegard GM, Clancy TC, Gates TS (2005) Polymer 46:553
4. Ragosta G, Abbate M, Musto P, Scarinzi G, Mascia L (2005) Polymer 46:10506
5. Mizutani T, Arai K, Miyamoto M, Kimura Y (2006) Prog Org Coat 55:276
6. Zheng K, Chen L, Li Y, Cui P (2004) Polym Eng Sci 44:1077
7. Chiang CL, Ma CCM (2004) Polym Degrad Stabil 83:207
8. Wang YW, Yen CT, Chen WC (2005) Polymer 46:6959
9. Wang Y, Wang X, Li J, Mo Z, Zhao X, Jing X, Wang F (2001) Adv Mater 13:1582
10. Salgueiriño-Maceira V, Correa-Duarte MA, Spasova M, Liz-Marzán LM, Farle M (2006) Adv Funct Mater 16:1266
11. Yu J, Guo ZX, Gao YF (2001) Macromol Rapid Commun 22:1261
12. Reculusa S, Mingotaud C, Bourgeat-Lami E, Duguet E, Ravaine S (2004) Nano Lett 4:1677
13. Luna-Xavier JL, Bourgeat-Lami E, Guyot A (2001) Colloid Polym Sci 279:947
14. Luna-Xavier JL, Guyot A, Bourgeat-Lami E (2001) J Colloid Interface Sci 250:82

15. Luna-Xavier JL, Guyot A, Bourgeat-Lami E (2004) Polym Int 53:609
16. Inoubli R, Dagréou S, Khoukh A, Roby F, Peyrelasse S, Billon L (2005) Polymer 46:2486
17. Bourgeat-Lami E, Espiard Ph, Guyot A (1995) Polymer 36:4385
18. Espiard Ph, Guyot A (1995) Polymer 36:4391
19. Zhang K, Chen HT, Chen X, Chen ZM, Cui ZC, Yang B (2003) Macromol Mater Eng 288:380
20. Li H, You B, Gu GX, Wu LM, Chen GD (2005) Polym Int 54:191
21. Lee CF, Tsai H, , Wang LY, Chen CF, Chiu WY (2005) J Polym Sci: Polym Chem 43:342
22. Reculusa S, Poncet-Legrand C, Ravaine S, Mingotaud C, Duguet E, Bourgeat-Lami E (2002) Chem Mater 14:2354
23. Chen M, Zhou SX, You B, Wu LM (2005) Macromolecules 38:6411
24. Percy MJ, Barthet C, Lobb JC, Khan MA, Lascelles SF, Vamvakaki M, Armes SP (2000) Langmuir 16:6913
25. Cheng XJ, Chen M, Zhou SX, WU LM (2006) J Polym Sci: Polym Chem 44:3807
26. Barthet C, Hickey A, , Cairns DB, Armes SP (1999) Adv Mater 11:408
27. Amalvy JI, Percy MJ, Armes SP (2001) Langmuir 17:4770
28. Mizetani T, Arai K, Miyamoto M, Kimura Y (2006) J Appl Polym Sci 99:659
29. Huang ZB, Tang FQ (2004) Acta Polymerica Sinica 6:835
30. Qi DM, Bao YZ, Huang ZM, Weng ZX (2006) J Appl Polym Sci 99:3425
31. Qi DM, Bao YZ, Weng ZX, Huang ZM (2006) Polymer 47:4622
32. Berendsen GE, de Galan L (1978) J Liq Chromatogr 1:1561
33. Vignati E, Piazza R (2003) Langmuir 19:6650